

Accepted Manuscript

Softening of POPC membranes by magainin

Hélène Bouvrais, Philippe Méléard, Tanja Pott, Knud J. Jensen, Jesper Brask, John H. Ipsen

PII: S0301-4622(08)00121-X  
DOI: doi: [10.1016/j.bpc.2008.06.004](https://doi.org/10.1016/j.bpc.2008.06.004)  
Reference: BIOCHE 5121

To appear in: *Biophysical Chemistry*

Received date: 28 March 2008  
Revised date: 2 June 2008  
Accepted date: 2 June 2008



Please cite this article as: Hélène Bouvrais, Philippe Méléard, Tanja Pott, Knud J. Jensen, Jesper Brask, John H. Ipsen, Softening of POPC membranes by magainin, *Biophysical Chemistry* (2008), doi: [10.1016/j.bpc.2008.06.004](https://doi.org/10.1016/j.bpc.2008.06.004)

This is a PDF file of an unedited manuscript that has been accepted for publication. As a service to our customers we are providing this early version of the manuscript. The manuscript will undergo copyediting, typesetting, and review of the resulting proof before it is published in its final form. Please note that during the production process errors may be discovered which could affect the content, and all legal disclaimers that apply to the journal pertain.

# Softening of POPC membranes by magainin

Hélène Bouvrais <sup>a,b</sup>, Philippe Méléard <sup>b</sup>, Tanja Pott <sup>b</sup>,

Knud J. Jensen <sup>c</sup>, Jesper Brask <sup>c</sup>, John H. Ipsen <sup>a,\*</sup>

<sup>a</sup>*Department of Physics and Chemistry, MEMPHYS-Center for Biomembrane*

*Physics, University of Southern Denmark, Odense, DK*

<sup>b</sup>*UMR-CNRS 6510, Université de Rennes 1, Rennes, FR*

<sup>c</sup>*Department of Natural Sciences, Section for Bioorganic Chemistry, University of*

*Copenhagen, Frederiksberg, DK*

---

## Abstract

Magainin 2 belongs to the family of peptides, which interacts with the lipid membranes. The present work deals with the effect of this peptide on the mechanical properties of 1-palmitoyl-2-oleoyl-*sn*-glycerol-3-phosphocholine Giant Unilamellar Vesicle, characterized by the bending stiffness modulus. The bending elastic modulus is measured by Vesicle Fluctuation Analysis at biologically relevant pH and physiological buffer conditions and shows a dramatic decrease with increasing peptide concentration. The observed bilayer softening is interpreted in terms of a continuum model describing perturbations on the membrane organization. Our analysis suggests that the adsorbed peptides give rise to considerable local curvature disruptions of the membrane.

### *Key words:*

Lipid bilayer, Vesicle Fluctuation Analysis, Membrane mechanics, Magainin, Bending elasticity, Continuum model

---

Since their discovery 20 years ago as components of the innate immune system of the African clawed frogs *Xenopus laevis* [1], magainins have been subject to intensive biophysical studies as model systems for the understanding of the interactions between antimicrobial peptides and biomembranes. Membranes are the likely target for the magainin actions because these peptides display a relatively unspecific and broadband antimicrobial activity [2] probably due to their amphipatic nature. More specifically, magainin 2 and its synthetic derivatives have been scrutinized. Magainin 2 consists of 23 amino acids with a net positive charge  $z=+4$  [3] under physiological conditions ( $z=3.6 - 3.8$  for the magainin 2-amide [4]). Numerous studies support the picture that magainins exhibit a random coil conformation in solution [5–7]. Adsorbed on membranes, they fold as  $\alpha$ -helices lying parallel on the bilayer surface, their hydrophobic residues being buried into one of the monolayers of the lipid bilayer structure [5–15]. At low adsorbed peptide densities, the helices are relatively spread on the surfaces [16], while at higher membrane concentrations, pore-like structures resulting from the aggregation of transmembrane oriented peptides has been shown on oriented lipid bilayers by X-ray, circular dichroism and NMR studies [15,17]. These properties are common to a variety of antimicrobial peptides including melittins, cecropins and ovispirins [18].

The precise mode of actions for the antimicrobial activity of magainin and similar antimicrobial peptides is still unclear. However, the observed membrane lytic activity on biological membranes and the pore forming ability of

---

\* Corresponding author

*Email address:* [ipsen@memphys.sdu.dk](mailto:ipsen@memphys.sdu.dk) (John H. Ipsen).

where magainins break down the barrier properties of the membrane. In particular, different models of pores through the membranes have been popular for the magainin, like the transmembrane helical bundles (analogous to the barrel stave model for the alamethicin) [21,22], the toroidal model [3,19], the carpet model [23,24] and the detergent like peptide model [25,26], for review see [27,28]. It has been challenging to prove that the antimicrobial action is linked to any of these models. Further, it is complicating the matter that the models are not mutually exclusive and may be applicable at different system conditions. For magainin, it is clear that the membrane barrier capacity is reduced by the presence of peptides in the membrane, while the data cannot support the formation of well-defined membrane channels.

In the present study, we have demonstrated that another material property of the membrane, the bending rigidity, is severely affected by the presence of magainin 2. By analysis of the flicker spectrum of Giant Unilamellar Vesicles (GUVs) under physiological buffer conditions, we show that the bending rigidity of POPC vesicles is dramatically reduced at  $\mu\text{M}$  bulk concentrations of magainin 2. Furthermore, by use of a model interpretation of the data in terms of a continuum description of the membrane, we gain important information about model parameters and the local and global effects of the peptide insertions into a membrane. This work represents to our knowledge the first material characterization of GUVs under physiological buffer conditions.

The paper is organized as follows. In Materials and Methods section, the peptide synthesis, the GUVs preparation under physiological buffer conditions and the technique of Vesicle Fluctuation Analysis (VFA) are presented. In the section Results and Discussion, the data from the measurements of the bending

rigidity are given and discussed, the effects of partitioning and electrostatics are treated and applied to our results. Finally, the data are interpreted in terms of a minimal continuum model describing the effects of peripheral peptides inclusions on membrane bending elasticity.

## Materials and Methods

### *Synthesis of magainin 2*

Magainin 2 was prepared by automated solid-phase peptide synthesis (SPPS) using Fmoc(9-fluorenylmethyloxycarbonyl)-amino acids. Amino acid symbols denote the L-configuration unless stated otherwise. All solvent ratios are volume/volume unless stated otherwise.

NovaSyn TG (Tentagel) resin and Fmoc-amino acids for peptide synthesis were from Novabiochem (Läufelfingen, Switzerland), HBTU (*N*-[(1*H*-benzotriazol-1-yl) (dimethylamino)methylene]-*N*-methylethanaminium hexafluorophosphate *N*-oxide) and HOBt (1-hydroxybenzotriazole) were from IRIS Biotech, while all other commercial compounds were purchased from Sigma-Aldrich (Copenhagen, Denmark). ESI-MS spectra were obtained on a Micromass LCT instrument (MassLynx software) by direct injection of an aqueous solution of the lyophilized product. HPLC analyses were carried out on a Waters system (600 control units, 996 PDA detectors, 717 Plus autosamplers, Millennium32 control software) equipped with either a Waters Symmetry300 C<sub>18</sub> 5  $\mu$ m column or a Waters Symmetry300 C<sub>4</sub> 5  $\mu$ m column, both 3.9  $\times$  150 mm. Preparative HPLC was carried out on a similar Waters system (with a Delta 600 pump) equipped either with a stack of three 40  $\times$  100 mm column car-

tridges of Waters Prep Nova-Pak HR C<sub>18</sub> 6  $\mu$ m 60 Å, or with a single 25  $\times$  100 mm column cartridge of Waters Delta-Pak HR C<sub>4</sub> 15  $\mu$ m 300 Å. Magainin 2 was eluted with mixtures of CH<sub>3</sub>CN and H<sub>2</sub>O, both containing 0.1% TFA (trifluoroacetic acid).

The magainin 2 sequence, H-Gly-Ile-Gly-Lys-Phe-Leu-His-Ser-Ala-Lys-Lys-Phe-Gly-Lys-Ala-Phe-Val-Gly-Glu-Ile-Met-Asn-Ser-OH, was assembled using a MilliGen 9050 PepSynthesizer starting with a FmocSer(*t*Bu)-Tentagel (NovaSyn TG resin, 0.50 g, 0.16 mol/g). Amino acids were coupled as their N <sup>$\alpha$</sup> -Fmoc protected derivatives; the following trifunctional amino acid derivatives were used: Fmoc-Ser(*t*Bu)-OH, Fmoc-Glu(*t*Bu)-OH, Fmoc-Lys(Boc)-OH, Fmoc-Asn(Trt)-OH and Fmoc-His(Trt)-OH. For each activation (coupling) step, 4 eqv. of Fmoc-amino acids, 3.8 eqv. of HBTU, 4 eqv. of HOBT and 8 eqv. of DIPEA (*N,N'*-diisopropylethylamine) were coupled for 30 minutes. However, Asn, Val and His, as well as the amino acids following these, were coupled for 60 minutes. Finally, the peptide was cleaved off with Reagent K, TFA-PheOH-H<sub>2</sub>O-PhSCH<sub>3</sub>-EDT (82.5:5:5:5:2.5, 8 mL) for 1 hour. The resin was filtered and washed with TFA (3  $\times$  5 mL), and the combined cleavage mixture and washings were concentrated to 2 mL, and precipitated with cold diethyl ether (35 mL). After centrifugation, the pellet was redissolved in TFA (2 mL) and re-precipitated with cold diethyl ether (35 mL), which was repeated twice. The precipitate was dissolved in H<sub>2</sub>O-CH<sub>3</sub>CN (1:1, 10 mL) and was purified by preparative C<sub>18</sub> RP-HPLC to give magainin 2 as a white powder after lyophilization. Yield 79 mg;  $\sim$  31% (included 6  $\times$  TFA). ESI-MS, calculated for C<sub>114</sub>H<sub>180</sub>N<sub>30</sub>O<sub>29</sub>S<sub>1</sub>: 2466.95 Da. Found:  $m/z$  1234.08 [M + 2H]<sup>2+</sup>, 823.22 [M + 3H]<sup>3+</sup>, 617.64 [M + 4H]<sup>4+</sup>.

POPC (1-palmitoyl-2-oleyl-*sn*-glycerol-3-phosphocholine) (purity > 98%) was obtained from Avanti Polar Lipids Inc. (Birmingham, Alabama, USA). Some MilliQ Water (Millipore, Bedford MA, USA) were added to the POPC powder to obtain a lipid concentration of about 0.2 mg/mL. The dispersion was agitated gently and the lipids hydrated for a few minutes. Then the dispersion was sonicated in order to obtain SUVs. For that step, a sonicator (Misonix sonicator 3000) was used: five sonications of two minutes were made at 70 W, with a break of five minutes between each sonication so that there was not too much heat transferred in the sample. The sonicated dispersion was filtered using a 0.2  $\mu$ m filter (sterile celluloseacetate membrane) to remove metal particles.

SUVs deposits were made on platinum wire electrodes (6 spots of 1.5  $\mu$ L on each electrode) using the sonicated dispersion prepared as previously described. The water was evaporated during several hours and during this step the electrodes were protected from the light. When the water has been evaporated, the electrodes were immersed in a magainin solution of high salinity: 100 mM of NaCl (sodium chloride) in order to be under conditions similar to the physiological ones, 10 mM of Tris (2-amino-2-hydroxymethyl-1,3-propanediol) adjusted to pH  $\approx$  7.4 and 2 mM of EDTA (ethylenediamine tetraacetic acid). NaCl (purity > 99.5%) was obtained from Fluka, Tris (ultra pure product) from Research Organics and EDTA (purity > 99.4%) from Sigma-Aldrich (Denmark). This buffer solution with varied concentrations of magainin was introduced in cells made of optical glass (Hellma), with a light path of 1 mm. The GUVs were formed by electroformation, but the standard

in order to obtain giant vesicles under physiological buffer conditions [31]. The big difference with the standard protocol was the frequency used during the electroformation, that is to say 500 Hz instead of 10 Hz. When the electrodes were connected, an electric field of 150 mV at 500 Hz was applied during 10 minutes by using a waveform generator (Agilent 33120A 15 MHz function). Then, the electric field at 500 Hz was increased until 1.35 V during 20 minutes and finally the electric field was pushed to 3.9 V for 90 minutes. Big vesicles with a diameter between 5 and 50  $\mu\text{m}$  were visible on the electrodes. At the end, both the frequency and the amplitude of the electric field were decreased to respectively 3 Hz and 1 V for 30 minutes in order to facilitate the removal of the vesicles from the electrodes.

#### *Vesicle fluctuation analysis*

Vesicles were observed directly in the electroformation cuvette, which was placed in a home custom made temperature controlled chamber holder (30  $^{\circ}\text{C}$ ). Vesicles were visualized using a phase contrast microscope (Axiovert S100 Zeiss, Göttingen, Germany), equipped with a  $\times 40/0.60$  objective (440865 LD Achroplan) and a magnification lens. The vesicle two-dimensional contour in the focal plane of the objective was thus obtained. A CCD Camera (SONY SSC-DC50AP) was used to capture a series of 3000 to 4000 contours in real time at a rate of 25 frames per second with a video integration time of 4 ms. Using home custom made softwares, the bending elastic modulus was obtained for a given system as an average of 10 to 30 vesicles with a diameter between 5 and 30  $\mu\text{m}$ .



elastic modulus of POPC/magainin 2 systems. Values of the bending elasticity were extracted from thermally induced shape undulations of the membrane. The shape of an homogeneous lipid bilayer is described by Helfrich's curvature free energy [32]:

$$F = \frac{\kappa}{2} \int_A dA \cdot \left( \frac{1}{r_1} + \frac{1}{r_2} - 2H_0 \right)^2 \quad (1)$$

where  $r_1$  and  $r_2$  are local curvature radii, and  $\kappa$  is the bending elastic modulus;  $H_0$  is the spontaneous curvature of the membrane, which reflects asymmetry in the composition of the two monolayer leaflets of the membrane. Due to the procedure used to form giant vesicles, we assume a complete symmetry in both monolayers, therefore  $H_0 = 0$ .

For each captured frame, the center of mass and the instantaneous vesicle contour in the focal plane are obtained and then the contour shape is characterized in polar coordinates  $r(\phi, t)$ . To quantify the shape thermal fluctuations, the angular correlation function of the relative radius fluctuations is calculated [33]:

$$\xi(\psi, t) = \frac{1}{R^2} \left( \left( \frac{1}{2\pi} \int_0^{2\pi} d\phi \cdot r(\phi + \psi, t) \cdot r(\phi, t) \right) - \left( \frac{1}{2\pi} \int_0^{2\pi} d\phi \cdot r(\phi, t) \right)^2 \right) \quad (2)$$

where  $R$  is the average radius of the contour.

By expanding  $\xi(\psi, t)$  using Legendre polynomials  $P_n(\cos\psi)$  ( $\xi(\psi, t) = \sum_n B_n(t) \cdot P_n(\cos\psi)$ ,  $n \geq 2$ ) and making time average of the amplitudes in the Legendre expansion  $\langle B_n \rangle_t$ , the spectrum of the shape fluctuations of the quasi-spherical vesicle is then obtained. The average of all coefficients,  $\langle B_n \rangle_t$ ,

$$\langle B_n(\kappa, \bar{\sigma}) \rangle = \frac{k_B T}{4\pi\kappa} \frac{2n+1}{(n+2)(n-1)(\bar{\sigma} + n(n+1))} \quad (3)$$

where  $n \geq 2$ . Here  $n$  is the Legendre mode number and,  $\kappa$  and  $\bar{\sigma}$  are fitting parameters obtained by a  $\chi^2$ -fit of the Eq. 3.  $\bar{\sigma}$  reflects the amount of surface excess area for the vesicle and is thus varying strongly between the vesicles.

Vesicles were selected when  $\chi_{min}^2 \approx f$ , where  $f = n_{max} - n_{min}$  is the number of degrees of freedom for the  $\chi^2$ -fit, and when  $\kappa$  and  $\bar{\sigma}$  were not excessively large.  $n_{min}$  and  $n_{max}$  are the lowest and highest modes to be considered in the analysis [34]. High  $\kappa$  values may indicate a multilamellar vesicle, while very large  $\bar{\sigma}$  values signal a tense membrane which may distort the analysis.

An alternative method in order to obtain the bending rigidity is the micropipette technique, where the low tension entropic elasticity yields information about the bending elastic modulus [35,37]. However for membranes with partitioning agents, the vesicle fluctuations technique is superior, since an applied tension severely perturbs the partitioning into a membrane.

## Results and Discussion

In this section, we will present and discuss the decrease in the observed bending rigidity of POPC-membranes in presence of magainin 2 and interpret the results in terms of membrane partitioning of magainin and its effects on the thermo-elasticity of bilayer membranes.

In this study, we investigate the physical perturbations induced by magainin 2 on the membrane. For that purpose the bending elasticity,  $\kappa$ , is a key parameter to describe membrane mechanical properties. The measurements of the bending elastic modulus made at 30 °C for each magainin concentration  $C_p^t$  allow us to see peptide effects on the membrane stability. The obtained  $\kappa$  values are displayed in Table 1. The value of  $\kappa$  without magainin is similar to the one obtained by Kučerka et al. with the X-Ray technique also for POPC bilayer, which was equal to  $0.85 \cdot 10^{-19}$  J [36].

In Fig. 1, we clearly see the decrease of the bending rigidity  $\kappa$  as a function of the total peptide concentration  $C_p^t$ . A decrease in the bending rigidity of lipid membranes at low peptide levels in pure water has also been reported for alamethicin from the fungus *Trichoderma viride* and for mellitin from the venom of the honey bee *Apis mellifera* [38,39]. This may indicate that the decrease in membrane rigidity is a characteristic of the interactions between membranes and these biomolecules.

It is noteworthy that the dramatic effects on membrane mechanical behavior observed here occur for very low peptide concentrations (micromolar range). Besides, this decrease of the bending rigidity indicates that the peptides cause a softening of the membrane bending resistance.

Our results for  $\kappa$  are plotted as a function of total concentrations of peptides (Fig. 1). But, the effects observed on the membranes mechanical properties are induced by the peptides bound to the lipid bilayers. Therefore the interesting concentration is that of the bound peptide,  $C_p^b$ . In order to know the  $C_p^b$  values, we need the partition coefficient  $K_p$ , which is defined according to:

$$\frac{C_p^b}{C_l} = K_p \cdot C_p^M \quad (4)$$

where  $C_p^M$  is the peptide concentration close to the membrane and  $C_l$  the lipid concentration of the samples.

Consequently, the peptide area coverage  $AC_p$ , parameter we choose in order to represent our experimental data, can be written:

$$AC_p = \frac{A_p^b}{A_{memb}} \approx \frac{A_p^b}{A_l} = \frac{C_p^b \cdot a_p}{C_l \cdot a_l} = \frac{K_p \cdot C_p^M \cdot a_p}{a_l} \quad (5)$$

where  $a_p$  and  $a_l$  are respectively the cross sectional area per peptide and per lipid equal to  $340 \text{ \AA}^2$  for the magainin 2 [17,40] and equal to  $64 \text{ \AA}^2$  for POPC [41].

Using a partitioning study previously published by Wieprecht et al., we can evaluate the peptide area coverage  $AC_p$  (Table 2) from their determined partition coefficient of magainin for POPC SUVs in buffer (10 mM Tris and 100 mM NaCl) at  $30^\circ\text{C}$  equal to  $2000 \text{ M}^{-1}$  [42].  $K_p$  was measured using the technique of isothermal titration calorimetry (ITC). The application of  $K_p$  value obtained from SUVs study is based on the observation that partition of amphipatic helices is similar for large and small vesicles [4,43].

determined the  $C_p^M$  concentrations for each  $C_p^t$  one involved [42]. Thus, we can correlate the  $C_p^t$  concentrations to  $AC_p$  percentages (Table 2). For the first concentrations, the differences between the  $C_p^M$  concentrations and the  $C_p^t$  ones are not so important, because we are in presence of zwitterionic POPC membranes, very low magainin concentrations and buffer solutions of high salinity leading to a maximum Debye length  $l_D \sim 10 \text{ \AA}$ , if we consider only the contribution of NaCl (screening effect). But, for the highest concentration, a major difference is noted due to the peptide adsorption on the membranes, leading to electric double layer effects.

Now, the bending elastic modulus  $\kappa$  can be plotted as a function of the peptide area coverage  $AC_p$  (Fig. 2). It appears thus clearly that magainin 2 effects on the bending rigidity are important for  $AC_p$  percentages inferior to 0.5%, corresponding to a big decrease of  $\kappa$  and for higher  $AC_p$  percentages, the magainin inclusions effects on  $\kappa$  seem to be less important, leading to a stabilization of the  $\kappa$  values.

### *Data modeling*

In this part, we will present a simple continuum model describing the effects of peripheral inclusions on membrane stability. It will account for the presence of inclusions in the membrane, which will affect the local membrane curvature and induce interactions between inclusions within the same monolayer and from opposite monolayers.

The shape of a simple, symmetric membrane is well described by Helfrich's

$$F_{Helf} = \frac{\kappa}{2} \int_A dA \cdot \left( \frac{1}{r_1} + \frac{1}{r_2} \right)^2 \quad (6)$$

In the very dilute limit, the distribution of inclusions on a flat membrane is well described by a 2-D ideal gas:

$$\begin{aligned} F_{Gas}^0 &= k_B T \int_A dA \cdot \left( \rho_{up} \cdot (\ln(\rho_{up} \cdot a^2) - 1) + \rho_{down} \cdot (\ln(\rho_{down} \cdot a^2) - 1) \right) + cst \\ &\approx \int_A dA \cdot \left( 2k_B T \cdot \rho_0 \cdot \ln(\rho_0 \cdot a^2) + k_B T \cdot \rho_0 \cdot \left( \frac{\Delta\rho}{2\rho_0} \right)^2 + cst \right) \end{aligned} \quad (7)$$

where  $\rho_{up} = \rho_0 - \Delta\rho/2$  and  $\rho_{down} = \rho_0 + \Delta\rho/2$  are respectively the local densities of peptides on the upper and lower monolayers, and  $a$  represents a molecular length scale in the membrane.  $\rho_0$  is the overall average density while  $\Delta\rho$  displays local variations around zero, since the two monolayers are symmetric. Eq. 7 is an expansion of  $F_{gas}^0$  up to  $2^{nd}$  order in  $\Delta\rho/\rho_0$ .

The interactions between inclusions are included as the lowest order virial correction to the ideal gas expression Eq. 7. There are two possible contributions:

- (1) The in-plane effective interactions between peptides within the monolayers:

$$F_{Gas}^1 = \frac{t}{2} \int_A dA \cdot (\rho_{up}^2 + \rho_{down}^2) = t \int_A dA \cdot \left( \rho_0^2 + \left( \frac{\Delta\rho}{2} \right)^2 \right) \quad (8)$$

Contributions to interaction parameter  $t$  can originate e.g. from the excluded volume effect  $t \sim a_{peptide} \cdot k_B T$  and from electrostatic interactions  $t \sim z^2 \cdot k_B T \cdot l_B l_D$ , with Bjerrum length  $l_B \sim 7 \text{ \AA}$ . Both of these contributions are repulsive and suggest  $t \approx 10^{-37} - 10^{-38} \text{ J.m}^2$  [44,45].

$$F_{Gas}^2 = s \int_A dA \cdot \rho_{up} \cdot \rho_{down} = s \int_A dA \cdot \left( \rho_0^2 - \left( \frac{\Delta\rho}{2} \right)^2 \right) \quad (9)$$

The effective interaction strength  $s$  between peptides locating on the two monolayer halves may involve electrostatics, Van der Waals forces and lipid packing effects.

There is no additional first virial corrections, which fulfill the up-down symmetry of the bilayer.

The final contribution to the free energy involves the coupling between the local shape of the membrane and the in-plane peptide distribution:

$$F_{Coupling} = \lambda \int_A dA \cdot \Delta\rho \cdot \left( \frac{1}{r_1} + \frac{1}{r_2} \right) \quad (10)$$

which is the simplest coupling term which respects the up-down symmetry.  $\lambda \cdot \Delta\rho$  can be understood as a local spontaneous curvature. This description of peripheral proteins insertion has previously been applied in the literature [46].

A simple stability analysis of the total free energy,  $F = F_{Helf} + F_{Gas}^0 + F_{Gas}^1 + F_{Gas}^2 + F_{Coupling}$ , reveals that thermo-mechanical stability of the vesicle is affected by the presence of inclusions. An important result relevant for our measurements is that the effective bending rigidity measured by VFA is modified according to:

$$\kappa^{\text{eff}} = \kappa - \frac{4\lambda^2 \cdot \rho_0 / k_B T}{1 + (t - s) \cdot \rho_0 / k_B T} \quad (11)$$

From Eq. 11, it follows that in the very dilute limit  $\rho_0 \ll k_B T / (t - s)$ ,  $\kappa^{\text{eff}}$  decreases linearly with the surface concentration  $\rho_0$ , where the slope  $4\lambda^2 / (k_B T)$

compositional asymmetry  $\Delta\rho$  between the monolayers. At higher concentrations  $\rho_0 > k_B T/(t-s)$ ,  $\kappa^{\text{eff}}$  behavior will depend on the sign of the expression  $(t-s)$ . If  $(t-s) > 0$ ,  $\kappa^{\text{eff}}$  may saturate at a value  $4\lambda^2/(t-s)$  lower than  $\kappa$ , while for  $(t-s) \leq 0$ ,  $\kappa^{\text{eff}}$  vanishes, destabilizing the vesicle (Fig. 2, insert).

The characteristic experimentally observed dependence of  $\kappa^{\text{eff}}$  on the peptide density  $\rho_0$  in the membrane (Fig. 2) can now be interpreted from the above model considerations. A fit to Eq. 11 predicts  $\lambda = 3.19 \pm 0.37 \cdot 10^{-28} \text{ J} \cdot \text{m}$  and  $(t-s) = 4.45 \pm 0.09 \cdot 10^{-36} \text{ J} \cdot \text{m}^2$ , shown in Fig. 2. In this dilute range of densities, these estimates are insensitive to the value of  $a_p$ .

The obtained value of the coupling parameter  $\lambda$  corresponds to a high local mean curvature,  $(\text{few nm})^{-1}$ . This leaves a picture of the membrane softening ability of magainin as originating from formation of local, mobile high-curvature spots on the membrane (Fig. 3). Such an estimate of  $\lambda$  due to peripheral inclusions has not been estimated from experimental data before. This coupling constant can in principle be calculated from lipid packing models [44,45].

The observed saturation of  $\kappa^{\text{eff}}$  with increasing peptide coverage of the membrane makes the estimate of  $(t-s)$  relatively large and positive. Unfortunately, it does not allow for an independent estimate of the two effective inter-peptide interaction parameters. If the in-plane interactions are dominated by contact interactions ( $t \sim \pm 10^{-38} \text{ J} \cdot \text{m}^2$ ), our estimate suggests significant effective intermonolayer attractive associations  $s \sim 10^{-36} \text{ J} \cdot \text{m}^2$ , which partially restore the local symmetry between the monolayers. The large magnitude of  $s$  cannot represent the direct intermolecular interactions between peptides on



the formation of temporal nanopores between monolayers [47].

## Conclusion

In the present study, we have conducted the first characterization of the material properties of GUVs at physiological buffer conditions. We have demonstrated that magainin 2 induces a substantial softening of POPC-bilayer vesicle reflected in the bending elastic modulus. The observed reduction in the bending stiffness is interpreted in terms of a continuum model involving coupling of peptides to membrane curvature, intra- and inter-monolayer peptide interactions, and information about model parameters are obtained from the experimental data. Our measurements and modeling leave a picture of magainins, inducing highly mobile regions with high curvature on the membrane surface, which soften the membrane and have some associations across the monolayers.

## Acknowledgments

The authors would like to thank Torben Sørensen for the building of the chamber holder. This work was made possible due to a collaboration between MEMPHYS - Center for Membrane Biophysics, supported by the Danish National Research Foundation, and the UMR-CNRS 6510, supported by the Centre National de la Recherche Scientifique. This study was also financed by the French Embassy in Denmark.

- [1] M. Zasloff, Magainins, a class of antimicrobial peptides from *Xenopus* skin: isolation, characterization of two active forms, and partial cDNA sequence of a precursor, *Proc. Natl. Acad. Sci. USA.* 44 (1987) 5449-5453.
- [2] M. Zasloff, B. Martin and H.C. Chen, Antimicrobial activity of synthetic magainin peptides and several analogues, *Proc. Natl. Acad. Sci. USA.* 85 (1988) 910-913.
- [3] K. Matsuzaki, Magainins as paradigm for the mode of action of pore forming polypeptides, *Biochim. Biophys. Acta.* 1376 (1998) 391-400.
- [4] T. Wieprecht, O. Apostolov and J. Seelig, Binding of the antibacterial peptide magainin 2 amide to small and large unilamellar vesicles, *Biophys. Chem.* 85 (2000) 187-198.
- [5] W.R. Williams, R. Starman, K. Taylor, K. Gable, T. Beeler, M. Zasloff and D. Covelle. Raman spectroscopy of synthetic antimicrobial frog peptide magainin 2a and PGLa, *Biochemistry.* 29 (1990) 4490-4496.
- [6] M. Jackson, H.H. Mantsch and J.H. Spence, Conformation of magainin-2 and related peptides in aqueous solution and membrane environments probed by Fourier transform infrared spectroscopy, *Biochemistry.* 31 (1992) 7289-7293.
- [7] T. Wieprecht, M. Dathe, M. Schümann, E. Krause, M. Beyermann and M. Bienert, Conformational and functional study of magainin 2 in model membrane environments using the new approach of systematic double-D-amino acid replacement, *Biochemistry.* 35 (1996) 10844-10853.
- [8] D. Marion, M. Zasloff and A. Bax, A two-dimensional NMR study of the antimicrobial peptide magainin 2, *FEBS Lett.* 227 (1998) 21-26.

Physicochemical determinants for the interactions of magainins 1 and 2 with acidic lipid bilayers, *Biochim. Biophys. Acta.* 1063 (1991) 162-170.

- [10] B. Bechinger, Y. Kim, L.E. Chirlian, J. Gesell, J.M. Neumann, M. Montal, J. Tomich, M. Zasloff and S.J. Opella, Orientations of amphipatic helical peptides in membrane bilayers determined by solid-state NMR spectroscopy, *J. Biomol. NMR.* 1 (1991) 167-173

- [11] B. Bechinger, M. Zasloff and S.J. Opella, Structure and interactions of magainin antibiotic peptides in lipid bilayers: a solid-state nuclear magnetic resonance investigation, *Biophys. J.* 62 (1992) 2-14.

- [12] B. Bechinger, M. Zasloff and S.J. Opella, Structure and orientation of the antibiotic magainin in membranes by solid-state nuclear magnetic resonance spectroscopy, *Protein Sci.* 2 (1993) 2077-2084.

- [13] M. Milik and J. Skolnick, Insertion of peptide chains into lipid membranes: an off-lattice Monte Carlo dynamics model, *Proteins.* 15 (1993) 10-25.

- [14] K. Matsuzaki, O. Murase, H. Tokuda, S. Funakoshi, N. Fujii and K. Miyajima. 1994. Orientational and aggregational states of magainin 2 in phospholipid bilayers, *Biochemistry.* 33 (1994) 3342-3349.

- [15] S.J. Ludtke, K. He, Y. Wu and H.W. Huang, Cooperative membrane insertion of magainin correlated with its cytolytic activity, *Biochim. Biophys. Acta.* 1190 (1994) 181-184.

- [16] M. Schümann, M. Dathe, T. Wieprecht, M. Beyermann and M. Bienert, The tendency of magainin to associate upon binding to phospholipid bilayers, *Biochemistry.* 36 (1997) 4345-4351.

- [17] S.J. Ludtke, K. He and H.W. Huang, Membrane thinning induced by magainin 2, *Biochemistry.* 34 (1995) 16764-16769.

(2003).

- [19] S.J. Ludtke, K. He, W.T. Heller, T.A. Harroun, L. Yang and H.W. Huang, Membrane pores induced by magainin, *Biochemistry*. 35 (1996) 13723-13728.

- [20] K. Matsuzaki, K. Sugishita, N. Ishibe, M. Ueha, S. Nakata, K. Miyajima and R.M. Epand, Relationship of membrane curvature to the formation of pores by magainin 2, *Biochemistry*. 37 (1998) 11856-11863.

- [21] M.S.P. Sansom, The biophysics of peptide models of ion channels. *Prog. Biophys. Mol. Biol.* 55 (1991) 139-235.

- [22] B. Bechinger, Structure and functions of channel-forming polypeptides: magainins, cecropins, melittin and alamethicin, *J. Membr. Biol.* 156 (1997) 197-211.

- [23] Y. Shai, Mechanism of binding, insertion and destabilization of phospholipid bilayer membranes by  $\alpha$ -helical antimicrobial and cell non-selective lytic peptides, *Biochim. Biophys. Acta*. 1462 (1999) 55-70.

- [24] Z. Oren and Y. Shai, Mode of action of linear amphiphatic  $\alpha$ -helical antimicrobial peptides, *Biopolymers*. 47 (1998) 451-463.

- [25] B. Bechinger, R. Kinder, M. Helmle, T.B. Vogt, U. Harzer and S. Schinzel, Peptide structural analysis by solid-state NMR spectroscopy, *Biopolymers*. 51 (1999) 174-190.

- [26] B. Bechinger, Detergent-like properties of magainin antibiotic peptides: a  $P^{31}$  solid-state NMR spectroscopy study, *Biochim. Biophys. Acta*. 1712 (2005) 101-108.

- [27] B. Bechinger, The structure, dynamics and orientation of antimicrobial peptides in membranes by multidimensional solid-state NMR spectroscopy, *Biochim. Biophys. Acta*. 1462 (1999) 157-183.

- [28] B. Bechinger and K. Lohner, Detergent-like actions of linear amphiphatic cationic antimicrobial peptides, *Biochim. Biophys. Acta.* 1758 (2006) 1529-1539.
- [29] M.I. Angelova and D.S. Dimitrov, Liposome electroformation, *Faraday Discuss. Chem. Soc.* 81 (1986) 303-311.
- [30] M.I. Angelova, S. Soléau, P. Méléard, J.F. Faucon and P. Bothorel, Preparation of giant vesicles by external AC electric fields. Kinetics and applications, *Prog. Colloid Polym. Sci.* 89 (1992) 127-131.
- [31] T. Pott, H. Bouvrais and P. Méléard. Giant unilamellar vesicle formation under physiological relevant conditions, *Chem. Phys. Lipids.* (2008) doi:10.1016/j.chemphyslip.2008.03.008.
- [32] W. Helfrich, Elastic properties of lipid bilayers: theory and possible experiments, *Z. Naturforsch.* 28 (1973) 693-703.
- [33] J.F. Faucon, M. Mitov, P. Méléard, I. Bivas and P. Bothorel, Bending elasticity and thermal fluctuations of lipid membranes. Theoretical and experimental requirements, *J. Physique.* 50 (1989) 2389-2414.
- [34] J.R. Henriksen, A. Rowat and J.H. Ipsen, Vesicle fluctuation analysis of the effects of sterols on membrane bending rigidity. *Eur. Biophys. J.* 33 (2004) 732-741.
- [35] E. Evans and W. Rawicz, Entropy-driven tension and bending elasticity in condensed-fluid membranes, *Phys. Rev. Lett.* 64 (1990) 2094-2097.
- [36] N. Kučerka, S. Tristram-Nagle and J.F. Nagle, Structure of fully hydrated fluid phase lipid bilayers with monounsaturated chains, *J. Membrane Biol.* 208 (2006) 193-202.
- [37] J.R. Henriksen and J.H. Ipsen, Measurements of membrane elasticity by micro-pipette aspiration, *Eur. Phys. J. E.* 14 (2004) 149-167.

- [38] V. Vitkova, P. Méléard, T. Pott and I. Bivas, Alamethicin influence on the membrane bending elasticity, *Eur. Biophys. J.* 35 (2006) 281-285.
- [39] C. Gerbeaud, Effet de l'insertion de protéines et de peptides membranaires sur les propriétés mécaniques et les changements morphologiques de vésicules géantes, Thèse, Université de Bordeaux I (1998).
- [40] C. Li and T. Salditt, Structure of magainin and alamethicin in model membranes studied by X-Ray reflectivity, *Biophys. J.* 91 (2006) 3285-3300.
- [41] G. Lantzsch, H. Binder and H. Heerklotz, Surface area per molecule in lipid/ $C_{12}E_n$  membranes as seen by fluorescence resonance energy transfer, *J. Fluoresc.* 4 (1994) 339-343.
- [42] T. Wieprecht, M. Beyermann and J. Seelig, Binding of antibacterial magainin peptides to electrically neutral membranes: thermodynamics and structure, *Biochemistry.* 38 (1999) 10377-10387.
- [43] J.A Gazzara, M.C. Philipps, S. Lund-Katz et al., Effect of vesicle size on their interaction with class A amphipathic helical peptides, *J. Lipid Res.* 38 (1997) 2147-2154.
- [44] A. Zemel, A. Ben-Shaul and S. May, Perturbation of a lipid membrane by amphipathic peptides and its role in pore formation, *Eur. Biophys. J.* 34 (2005) 230-242.
- [45] A. Zemel, A. Ben-Shaul and S. May, Membrane perturbation induced by interfacially adsorbed peptides, *Biophys. J.* 86 (2004) 3607-3619.
- [46] S. Leibler, Curvature instability in membranes, *J. Physique* 47 (1986) 507-516.
- [47] H. Leontiadou, A.E. Mark and S.J. Marrink, Antimicrobial peptides in action, *J. Am. Chem. Soc.* 128 (2006) 12156-12161.

*Figure 1*

Fig. 1. Experimental decrease of the bending elasticity  $\kappa$  as a function of the magainin 2 concentrations  $C_p^t$ . The measurements were made at 30 °C.

*Figure 2*

Fig. 2. Comparison between the experimental decrease of the bending elasticity  $\kappa$  at 30 °C as a function of the peptide area coverage  $AC_p$  (data point) and a theoretical one (continuous line) for which  $\lambda = 3.19 \pm 0.37 \cdot 10^{-28} \text{ J} \cdot \text{m}$  and  $(t - s) = 4.45 \pm 0.09 \cdot 10^{-36} \text{ J} \cdot \text{m}^2$ . In insert, comparison between different theoretical behaviors of  $\kappa$  for various values of  $(t - s)$ : continuous line for  $(t - s) > 0$ , dotted line for  $(t - s) = 0$  and dashed line for  $(t - s) < 0$ .

*Figure 3*

Fig. 3. A cartoon of the effect of a  $\alpha$ -helix insertion on the lipid packing.

Figure 1

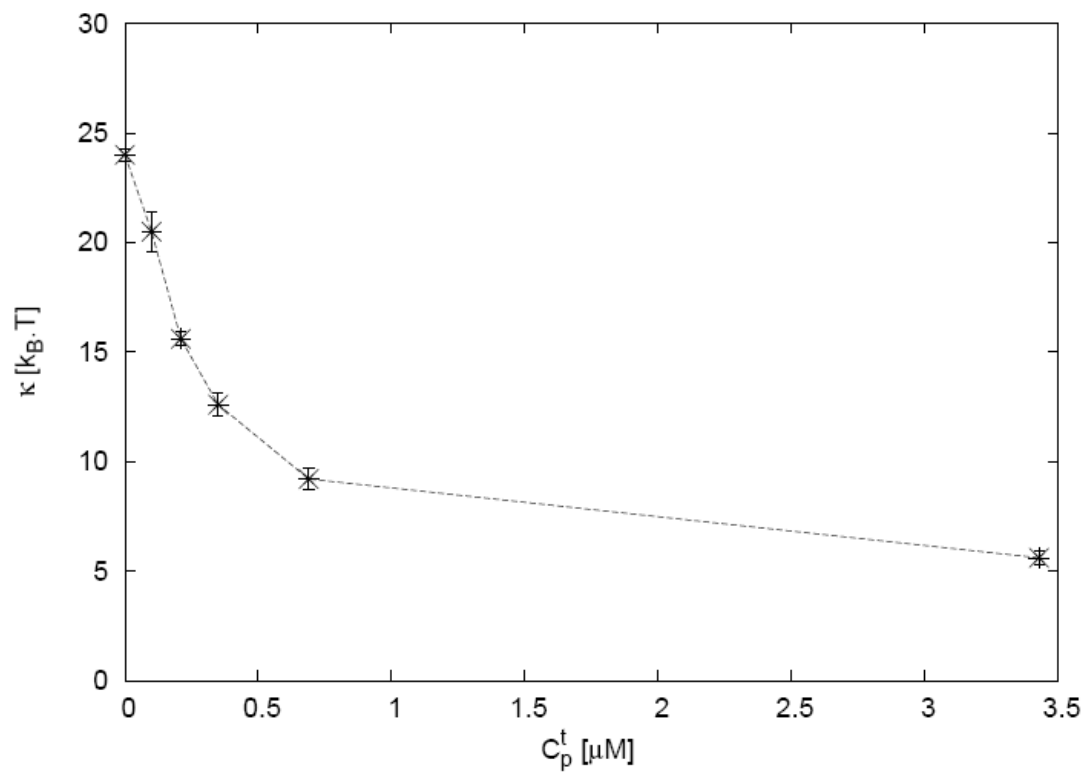




Figure 2

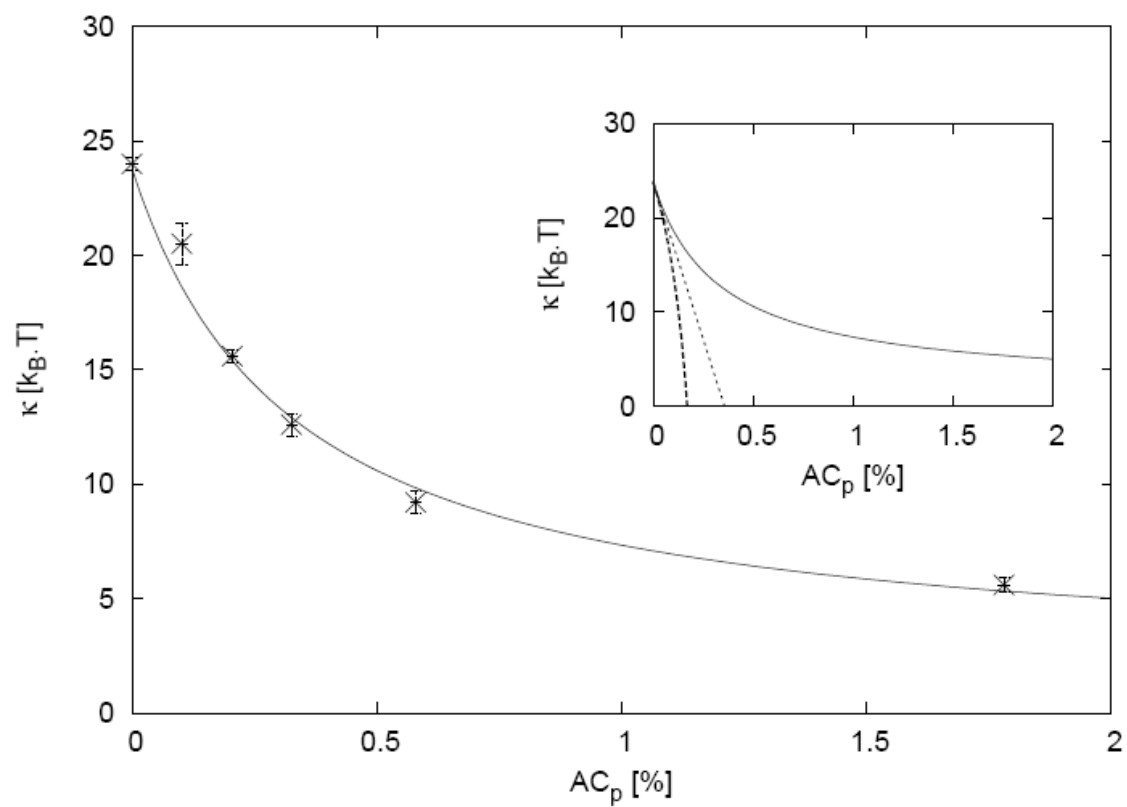
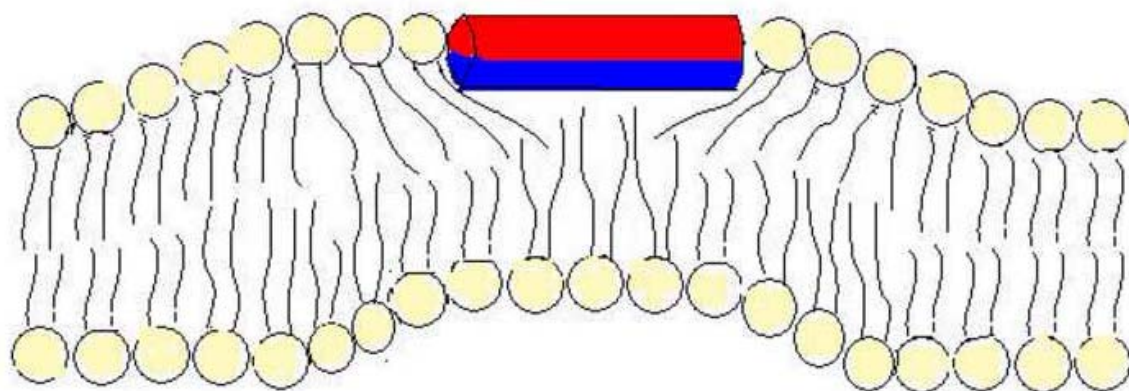


Figure 3



$C_p^t$ [ $\mu\text{M}$ ]	$\kappa$ [ $k_B T$ ]
0	$24.0 \pm 0.3$
0.10	$20.5 \pm 0.9$
0.21	$15.6 \pm 0.3$
0.35	$12.6 \pm 0.5$
0.69	$9.2 \pm 0.5$
3.43	$5.6 \pm 0.3$

Table 1

Effects of magainin 2 on POPC membranes at 30°C. Values of membrane bending rigidity,  $\kappa$ , were measured by flicker analysis. Error on  $\kappa$  represents standard deviation from the mean value of a vesicle population.

$C_p^t$ [ $\mu$ M]	$C_p^M$ [ $\mu$ M]	AC <sub>p</sub> [%]
0	0	0
0.10	0.096	0.102
0.21	0.193	0.205
0.35	0.307	0.326
0.69	0.546	0.580
3.43	1.677	1.782

Table 2

Correlation between the concentrations of magainin  $C_p^t$  and  $C_p^M$  and the magainin area coverage percentages of the membranes AC<sub>p</sub>.